International Journal of Petroleum and Petrochemical Engineering (IJPPE)
Volume 4, Issue 1, 2018, PP 55-69
ISSN 2454-7980 (Online)
DOI: http://dx.doi.org/10.20431/2454-7980.0401007
www.arcjournals.org

Petrophysical Analysis of Sylhet Gas Field Using Well Logs and Associated Data from Well Sylhet #, Bangladesh

Abdullah Al Fatta[1], Md. Shofiqul Islam[1], Md. Farhaduzzaman[2]

[1]*Department of Petroleum & Mining Engineering, Shahjalal University of Science & Technology, Sylhet, Bangladesh*

[2]*Petroleum Engineering Department, Sylhet Gas Fields Limited (A company of Petrobangla), Sylhet, Bangladesh*

Corresponding Author:** ***Md. Shofiqul Islam, *Department of Petroleum & Mining Engineering, Shahjalal University of Science & Technology, Sylhet, Bangladesh*

Abstract: *The present study has been conducted to evaluate the petrophysical properties of Sylhet Gas Field based on different logs data such as gamma-ray, spontaneous potential, density, neutron, resistivity, caliper and sonic logs. Quantitative properties including shale volume, porosity, permeability, fluid saturation, HC movability index and bulk volume of water were carried out using the well logs. Fourteen permeable zones were identified where six zones were found gas-bearing, one was oil bearing and the rest were water bearing. Computed petrophysical parameters across the reservoir provided average porosity as ranging from 16 to 26%, the permeability values range from 52 to 349 mili Darcy (mD) and the average hydrocarbon saturations are 75%, 68%, 77%, 76%, 63%, 73%, and 63% for reservoir Zone 1, Zone 2, Zone 3, Zone 4, Zone 5, Zone 6 and Zone 7 respectively. Hydrocarbon was found moveable in the reservoir since all the hydrocarbon movability index value was less than 0.70. An average bulk volume of water ranged from 0.04 to 0.08. Analyzed data indicate that the reservoirs are sandstone dominating with minor amount of shale and are at irreducible water saturation. The petrophysical parameters supported a hydrocarbon reservoir with good to very good quality which provide satisfactory hydrocarbon production.*

Keywords: *Sylhet Gas Field, Surma Basin, Petrophysical analysis, Porosity, Permeability, HC saturation*

1. Introduction

Reservoir characterization involves the integration of a vast amount of seismic data, geophysical well logs and geological samples [1]. The oil and gas industry uses wireline logs to obtain a continuous record of a formation's rock properties. Petrophysical evaluation has a unique opportunity to observe the relationship between porosity and saturation [2]. The determinations of reservoir quality and formation evaluation processes are largely depended on quantitative evaluation of petrophysical analysis. It becomes necessary therefore, to know the complete reservoir architecture of the reservoir which includes the internal and external geometry, its model, as well as the distribution of the reservoir properties. These reservoir properties are classified into two groups, viz.: static (such as porosity, permeability, heterogeneity, net pay, and thickness) and dynamic (fluid flow within the reservoir) [3].

Petrophysical log interpretation is one of the most useful and important tools to characterize the reservoir property [4]. Well log data helps to identify permeable zones and productive zones for hydrocarbon. It distinguishes the interfaces of oil, gas or water of a particular reservoir. Permeable zones may contain either hydrocarbon or water or both. Petrophysical study involves the analysis of different parameters of reservoirs including lithology, volume of shale, porosity, water saturation, hydrocarbon saturation, permeability, hydrocarbon movability and pore geometry by using appropriate well log data.

The Sylhet Gas Field is the only oil and gas producing field of Bangladesh which is located in the northern-east of the Sylhet city of the country (Fig. 1). It was the first discovery of hydrocarbon in Bangladesh. The Sylhet structure was delineated by Pakistan Petroleum Limited (PPL) after recording single fold seismic. Gas was discovered in 1955 by drilling the Sylhet-1 well, which was the first gas discovery well in Bangladesh. Unfortunately, the well blew out leaving a crater. Subsequently five more wells, Sylhet-2 to Sylhet-6, were drilled from 1956 to 1964. Sylhet-4 blew out on reaching 315 m and Sylhet-5 was drilled in 1963 as an observation well to a depth of 575 m. Sylhet-6 was drilled in 1964 to a depth of 1,405 m and completed as a dual producer.

Sylhet-7 was drilled in 1986 as a gas development well but turned out to be the first oil discovery well. Surma-1 and the sidetracked well Surma 1A were drilled in 1989 to appraise the oil discovery [5].

A master thesis work had been conducted at PMRE, BUET on reservoir simulation using production data analysis and pressure transient analysis for future production performance [Nath, 2010]. However, there is no works had been conducted on reservoir properties analysis using wireline logs and associated data. We aimed to evaluate the petrophysical characterization of the reservoir rocks including the porosity, permeability, water saturation, hydrocarbon saturation of the well Sylhet # of the Sylhet Gas Field.

2. Geologic Setting

Bangladesh lies in the northeastern corner of Indian subcontinent at the head of the Bay of Bengal [6]. Bengal Basin of Bangladesh is a young prolific depositional basin in the world [7]. This basin meets the entire geological requirement for accumulation of natural gas in the subsurface [8]. Sylhet Trough (Surma Basin) covers the northeastern part of the Bengal Basin, representing a promising petroleum bearing basin in the Southeast Asia [9].

The Sylhet Gas Field is located in the Surma Basin, which is a Miocene gas producing province in the north-eastern part of Bangladesh. In the Surma Basin, which forms a part of the Bengal Basin that subsided mainly from Oligocene to Pliocene, there deposited almost exclusive clastic sequences of deltaic to fluvial, and to a lesser degree marine sandstone, siltstone, and shale. These sediments were subjected to the later phases of the Himalayan Arakan Orogeny, resulting in the formation of the relatively gentle folds of the frontal folded belt [5].

The Surma Basin was formed structurally by the contemporaneous interaction of two major tectonic elements; the emerging Shillong Massive to the North and the westward moving mobile Indo-Burma Fold Belt. The tectonic movement is considered to have occurred from the Neogene to the present, with the strongest period of crustal disturbance during the middle Miocene. The primary result of these tectonics is a series of North-South oriented asymmetrical anticlines in Eastern Bangladesh, in which the degree of deformation increases eastward. Basin relief, structural elements, growth rate, style of traps, source rocks and maturities are suitable for forming gas-bearing structures of commercial size [5].

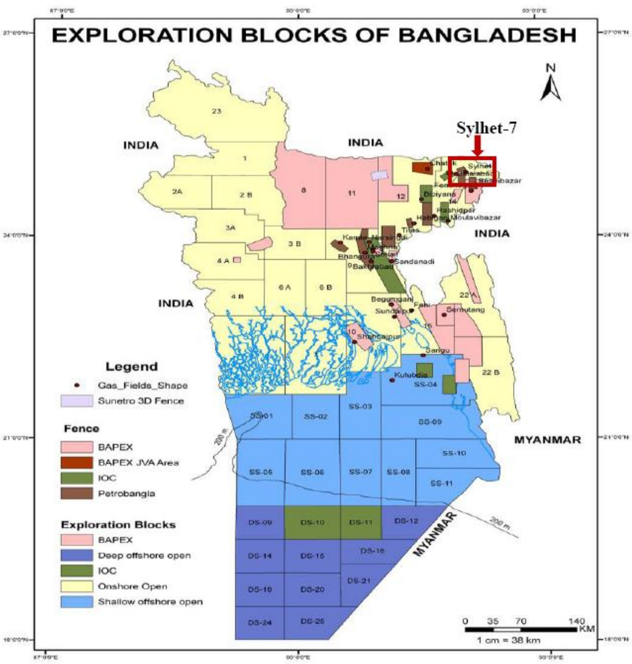

Fig1. *Geological map of Bangladesh. Showing the location of well Sylhet #* [10]

3. MATERIALS AND METHOD

Data for this present study were collected from the Sylhet Gas Field Limited (A Company of Petrobangla) with proper permission. The photocopy of the image of gamma ray (GR), resistivity (deep, medium and shallow), sonic, SP, neutron, density, bit size and caliper logs of well Sylhet # and some associated reports of that well were collected. The photocopy of the image of the logs were converted to images (TIFF format) by scanning. The scanned TIFF images were then converted to digital (text format) data by using the GetData Graph Digitizer 2.26 and Didger 3 software. The digital data also then transferred to Excel 2016 software for the analysis. The log values, lithology and calculated parameters were graphically represented and interpreted using Strater 2.5.704 and Adobe Illustrator software.

3.1. Formation Temperature Determination

Formation temperature (T_f) is important in log analysis, because the resistivity of the drilling mud (R_m), the mud filtrate (R_{mf}), and the formation water (R_w) vary with temperature [11]. We followed the western Atlas Logging Services, 1985, to determine the formation temperature as follows,

$$T_f = \left(\frac{BHT - AMST}{TD} \times FD \right) + AMST \tag{1}$$

Where,

AMST = Annual Mean Surface Temperature, BHT = Bottom Hole Temperature, FD = Formation Depth, T_f = Formation temperature.

3.2. Water Resistivity Determination

Formation water resistivity (R_w) of the hydrocarbon bearing zone was calculated by the following method [12],

$$R_w = \frac{R_{we} + 0.131 \times 10^{\left(\frac{1}{\log\left(\frac{T_f}{19.9}\right)} \right)^{-2}}}{-.5 \times R_{we} + 10^{\left(\frac{0.0426}{\log(T_f/50.8)} \right)}} \tag{2}$$

Where, $R_{we} = R_{mf} \times 10^{\frac{ssp}{(61+0.133T_f)}}$ (3)

$$R_{mf} = R_{mfs} \times \left(\frac{T_{ms} + 6.77}{T_f + 6.77} \right) \tag{4}$$

R_w=Water Resistivity, R_{mf} =Resistivity of Mud Filtrate.

3.3. Shale Volume Determination

Shale volume was determined by using the gamma ray index from a gamma ray log [11] and then shale volume was determined according to Larionov (1969) formula for Tertiary rocks,

$$I_{GR} = \frac{GR_{\log} - GR_{\min}}{GR_{\max} - GR_{\min}} \tag{5}$$

Where,
I_{GR} = Gamma ray index, GR_{log} = Gamma ray reading of formation, GR_{min} = Minimum gamma ray (clean sand or carbonate), GR_{max} = Maximum gamma ray (shale).

Larionov (1969) for Tertiary rocks,

$$V_{sh} = 0.083 \times (2^{3.7 * I_{GR}} - 1) \tag{6}$$

3.4. Porosity Determination from Porosity Logs

The porosity was determined by using the Sonic Log with Wyllie time-average equation [13],

$$\Phi_s = \frac{\Delta t_{\log} - \Delta t_{ma}}{\Delta t_{fl} - \Delta t_{ma}} \quad (7)$$

Where, Φ_s= Sonic-derived porosity, Δt_{ma} = Interval transit time in the matrix (Sandstone= 55.5 µsec/ft), $\Delta t_{\log}$ = Interval transit time in the formation, Δt_{fl} = Interval transit time in the fluid in the formation (freshwater mud = 189 µsec/ft).

Correction for Shale effect also conducted using the sonic log according to the equation [14],

$$\Phi_{se} = \left(\frac{\Delta t_{\log} - \Delta t_{ma}}{\Delta t_{fl} - \Delta t_{ma}} \times \frac{1}{C_p} \right) - V_{sh} \left(\frac{\Delta t_{sh} - \Delta t_{ma}}{\Delta t_{fl} - \Delta t_{ma}} \right) \quad (8)$$

The hydrocarbon effect was corrected by using the following empirical formula by Hilchie (1978) [11].

$$\Phi_s = \Phi \times 0.7 \text{ (Gas)} \quad (9)$$

$$\Phi_s = \Phi \times 0.8 \text{ (Oil)} \quad (10)$$

3.5. Density Porosity

The porosity was also calculated by the following formula according to [11]:

$$\Phi_D = \frac{\rho_{ma} - \rho_b}{\rho_{ma} - \rho_{fl}} \quad (11)$$

Where,
Φ_D = density derived porosity, ρ_{ma} = matrix density (Sandstone = 2.644 g/cm^3), ρ_b = formation bulk density (the log reading), ρ_{fl} = fluid density (Fresh water=1 g/cm^3).

For Shaly Formation, the porosity using the density log was calculated by the formula of [15],

$$\Phi_{De} = \Phi_D - \left[\left(\frac{\Phi_{Nshale}}{0.45} \right) \times 0.13 \times V_{Shale} \right] \quad (12)$$

3.6. Neutron Log

Neutron logs are porosity logs that measure the hydrogen concentration in a formation. In clean formations (i.e., shale-free) where the porosity is filled with water or oil, the neutron log measures liquid filled porosity (Φ_N, PHIN, or NPHI) [11].

For Shale effect, the porosity using the neutron log is [15],

$$\Phi_{Ne} = \Phi_N - \left[\left(\frac{\Phi_{Nshale}}{0.45} \right) \times 0.03 \times V_{Shale} \right] \quad (13)$$

3.7. Combined Porosity

By using density porosity and neutron porosity measurement pairs above, the combined porosity was calculated as [11],

$$\Phi_{ND} = \sqrt{\frac{\Phi_{Ne}^2 + \Phi_{De}^2}{2}} \quad (14)$$

Where, Φ_{ND} = Neutron-density shale-corrected porosity, Φ_{Ne} = Shale-corrected neutron porosity, Φ_{De} = Shale-corrected density porosity

3.8. Water Saturation Determination

Water Saturation is the amount of pore volume in a rock that is occupied by formation water. After the shale-corrected porosity has been determined, the water saturation can be calculated. A variety of techniques are being used to determine the water saturation determination [11]. In this study, Fertl (1975), Schlumberger (1975), Simandoux (1963) formula were used to evaluate the water saturation. They are as follows, Fertl, 1975 [16]:

$$S_w = \frac{1}{\Phi} \times \left[\sqrt{\frac{R_w}{R_t} + \left(\frac{a \times V_{sh}}{2} \right)^2} - \frac{a \times V_{sh}}{2} \right] \quad (15)$$

Schlumberger, 1975 [15]:

$$S_w = \frac{\sqrt{\left(\frac{V_{Sh}}{R_{sh}} \right)^2 + \frac{\Phi^2}{0.2 \times R_w \times (1.0 - V_{sh}) \times R_t}}}{\frac{\Phi^2}{0.4 \times R_w \times (1.0 - V_{sh})}} \quad (16)$$

Simandoux, 1963 [17]:

$$S_w = \left(\frac{0.4 \times R_w}{\Phi^2} \right) \times \left[\sqrt{\left(\frac{V_{sh}}{R_{sh}} \right)^2 + \frac{5 \times \Phi^2}{R_t \times R_w}} - \frac{V_{sh}}{R_{sh}} \right] \quad (17)$$

3.9. Bulk Volume of Water

The product of a formation's water saturation (S_w) and its porosity (φ) is the bulk volume of water (BVW) [11].

$$\mathrm{BVW} = \mathrm{S_W} \times \Phi \quad (18)$$

Where,
BVW = Bulk volume water, S_w = Water saturation of uninvaded zone, Φ= Porosity

3.10. The moveable hydrocarbon index

The moveable hydrocarbon index by the ratio method is [11],

$$\frac{S_w}{S_{xo}} = \left(\frac{R_{xo}/R_t}{R_{mf}/R_w} \right)^{\frac{1}{2}} \quad (19)$$

Where,

S_w/S_{xo} = Moveable hydrocarbon index, R_{xo} = Shallow resistivity from measurements such as laterolog-8, microspherically focused log, or microlaterolog, R_t = True formation resistivity (i.e., deep induction or deep laterolog corrected for invasion), R_{mf} = Resistivity of mud filtrate at formation temperature.

3.11. Permeability Determination

Permeability was calculated using the following formulas,

Wyllie and Rose [18]:

$$K = \left(250 \times \frac{\Phi^3}{S_{wirr}} \right)^2 \text{ (Medium gravity oils)} \quad (20)$$

$$K = \left(79 \times \frac{\Phi^3}{S_{wirr}} \right)^2 \text{ (Dry gas)} \quad (21)$$

Where,
K = Permeability in millidarcy, φ = Porosity, $S_{w\ irr}$ = Water saturation (S_w) of a zone at irreducible water saturation.

Timur [19]:

$$K = \left(\frac{93 \times \Phi^{2.2}}{S_{wirr}} \right)^2 \quad (22)$$

Coates and Dumanoir [20]:

A first step in the Coates and Dumanoir permeability formula is calculation of values for two constants: C and W [11].

$$C=23+465\times\rho_h-188\times \rho_h^2) \tag{23}$$

Where,

C = constant in Coates and Dumanoir permeability formula, ρ_h = hydrocarbon density in g/cm3

$$W=\left\{(3.75-\Phi)+\left[\frac{(\log(R_w/R_{tirr})+2.2)^2}{2}\right]\right\}^{\frac{1}{2}} \tag{24}$$

Where,

W = Constant in Coates and Dumanoir permeability formula, φ = Porosity, R_w = Formation water resistivity at formation temperature, $R_{t\ irr}$ = Deep resistivity from a zone at irreducible water saturation ($S_{w\ irr}$).

Once determined, the constants C and W can be used to calculate permeability.

$$K=\left[\frac{C\times\Phi^{2W}}{W^4\times(R_w/R_{tirr})}\right]^2 \tag{25}$$

Where,

K = Permeability in millidarcy (md), C = Constant based on hydrocarbon density, W = Constant, φ = Porosity,

$R_{t\ irr}$ = Deep resistivity from a zone at irreducible water saturation ($S_{w\ irr}$), R_w = Formation water resistivity at formation temperature.

4. Results And Discussions

4.1. Lithology of the Well

The petrophysical techniques are also invaluable methods for mapping and identifying lithologies. The lithology can be interpreted through using gamma ray (GR), spontaneous potential (SP), resistivity (LLD and LLS), and density log (RHOB) [21]. However, the lithology of different strata is also can be determined on the basis of reference values of density, gamma ray and resistivity of different rock types [7]. Moreover, there are many techniques that can assist geologists with lithologic determination and mapping such as the Neutron-density lithology plot, Neutron-sonic lithology plot, Density-sonic lithology plot, M-N lithology plot, Matrix identification plot (ρ_{maa} vs. Δt_{maa}) etc. Schlumberger Neutron-density cross-plot and Neutron-sonic lithology plot were used for lithology determination.

The gamma ray log was used to map clean (shale-free) sandstones vs. shaly sandstones and carbonates. Shale exhibited relatively high GR count rates due to presence of potassium ions in the lattice structure of clay mineral. On the other hand, reservoir rock (calcite, dolomite, quartz) exhibited relatively low GR count rates [22]. In the sandstone zones, the average gamma ray value ranges from 60-82 API (Fig. 4.3), which indicates the presence of sandstone. In shale zones, GR exhibits relatively high value where in mixed zones it is in medium range (Fig. 4.3).

The spontaneous potential (SP) log was also used to map clean (shale-free) sands vs. shaly sands. The technique is called alpha (α) mapping [23] where the presence of shale in a formation decreases the SP response. They were very negative in the sandstone zones showing an average SP values ranged from -61 to 18 mV (Fig. 4.3). In the shale zones, the deflection was very negative to positive (Fig. 4.3).

Using the SP, GR and resistivity log, a total nine sandstone zones and seven shale zones were identified for the well Sylhet #, Sylhet Gas Field (Fig. 4.1). There are three sand-shale mixed zones were also identified (Fig. 4.1).

Moreover, a lithology cross-plot between density-neutron porosity log of the data from the well Sylhet # is illustrated in the Fig. 4.2a. This cross-plot is usually used to differentiate between the common reservoir rocks [quartz sandstone, calcite and dolomite] and shale and some evaporates. It is clearly observed that most of the points of seven potential reservoir zones fall in the sandstone line zone and very few point lies between sandstone and limestone line except the Zone-7 which falls between dolomite and limestone line zone because of the presence of the shale (Fig. 4.2a). Another cross-plot between the sonic-neutron log was used to differentiate between the common reservoir rocks when clay content was negligible (Fig. 4.2b). It was also used to differentiate between a single known reservoir rock and shale and to identify evaporate minerals. The values of neutron porosity was entered on the x-axis and the sonic slowness (Δt) were entered on the y-axis to find their intersection point, which described the cross-plot porosity and the lithology composition of the formation. It is clear that the potential reservoir zones are sandstone dominated and a very few amounts of other compositions are also present in the sandstone zones (Fig. 4.2b).

The reservoir rock the gas field is mainly sandstones of Bokabil and upper Bhuban Formation was deposited under repeated transgressions and regressions of Miocene time. The Bokabil formation usually consists of fine to medium–grained sandstones with alternating mudstone or siltstone. The middle part of the Bokabil is more are naceous deposited under deltaic to shallow marine settings exposed throughout the south – east fold belt of Bengal basin and forms natural gas reservoirs in in the Bengal basin (Uddin & Lundberg, 1999). Deposition of reservoir rocks were occurred in fluvial deltaic to estuarine environments. The tectonics and geological setting of the study area have been greatly influenced by late Himalayan collision phase (Curiale et al., 2002).

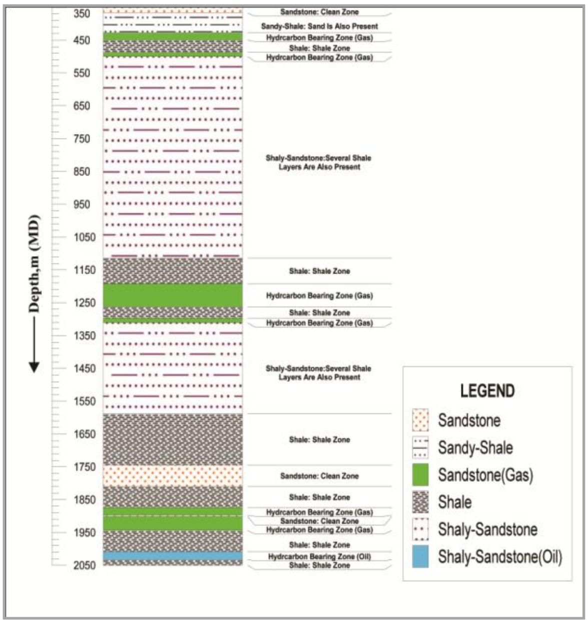

Fig4.1. *Lithology of different formations of the well Sylhet-#*

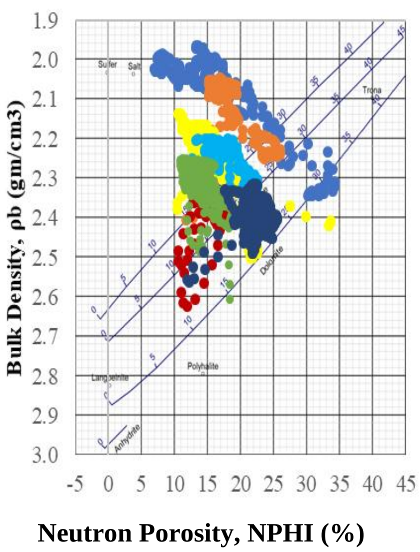

Fig4.2a. *Density-Neutron cross-plot for lithology and porosity determination, in case of fresh water, liquid-filled boreholes (after Schlumberger)* [24].

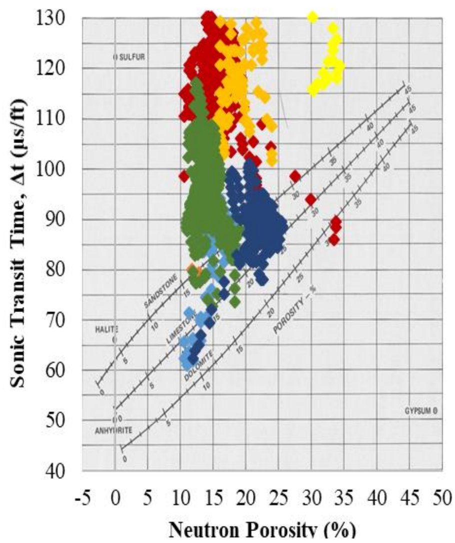

Fig. 4.2b *Sonic-Neutron cross-plot for lithology determination (after Schlumberger)* [24].

4.2. Permeable Zones in the well

Hydrocarbon-bearing zones in the well Sylhet-# were identified with the help of SP, GR, resistivity (deep resistivity log (ILD) & shallow resistivity log (MSFL)), sonic, neutron and density log responses. For this purpose, resistivity logs are the best option to detect gas-bearing zones [6]. Seven (07) hydrocarbon bearing zones were identified in which six were gas-bearing and one was oil-bearing zone (Table 4.1). Graphical representation of composite log response of Zone-3 (depth between 1192 to 1263 m) is shown in Fig. 4.3. Other zones can also be represented similarly (not shown). In these six gas-bearing zones, gamma ray log showed low response and SP log showed high values as these deflects from shale base line (Fig. 4.3). The resistivity log response in the gas-bearing zones was very high (Fig. 4.3). In these gas bearing zones, the ILD value was higher than the MSFL (Fig. 4.3). Very low neutron and low density log responses support that hydrocarbon are gas type [11]**.** This is a Neutron-density crossover. In water bearing zones the ILD value was lower than the MSFL or medium resistivity log (LL-3) (Fig. 4.3).

Table4.1. *Permeable Zones of the Well Sylhet #*

Depth Range (m) (MD)	Zone Type	Thickness (m)	Remark
428-450	Hydrocarbon Bearing	22	Zone-1
488-500	Hydrocarbon Bearing	12	Zone-2
850-875	Water Bearing	25	
1083-1113	Water Bearing	30	
1192-1263	Hydrocarbon Bearing	71	Zone-3
1297-1311	Hydrocarbon Bearing	14	Zone-4
1311-1321	Water Bearing	10	
1560-1590	Water Bearing	30	
1621-1640	Water Bearing	19	
1740-1800	Water Bearing	60	
1874-1898	Hydrocarbon Bearing	24	Zone-5
1901-1944	Hydrocarbon Bearing	43	Zone-6
1944-2009	Water Bearing	65	
2009-2033	Hydrocarbon Bearing	24	Zone-7

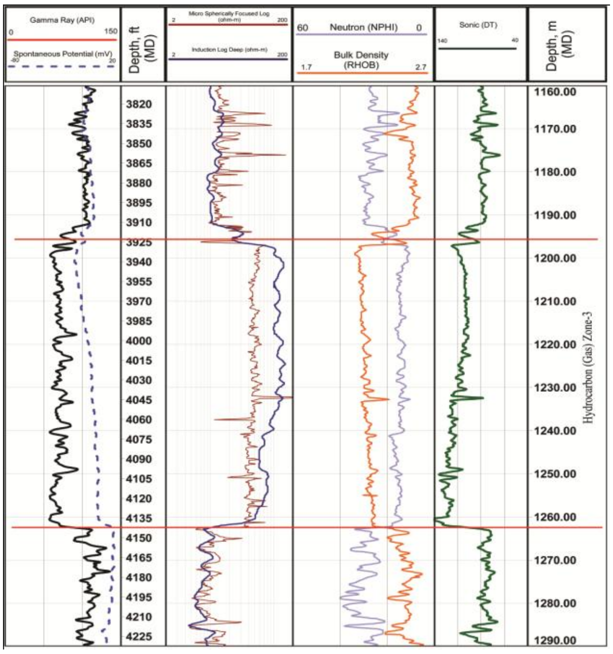

Fig4.3. *Composite log response of Zone-3(Gas) of well Sylhet #*

Table4.2. *Different Log Parameters and their Average Values Calculated from the HC Bearing Zones of the Well Sylhet #*

HC Zones	Depth, m (MD)	GR (API)	RILD (Ohm-m)	MSFL (Ohm-m)	Sonic, ΔT (ms/ft)	RHOB (g/cc)	NPHI (%)

Zone-1	428-450	85	71	36	164	2.1	16
Zone-2	488-500	79	54	32	161	2.1	19
Zone-3	1194-1263	70	95	46	115	2.2	15
Zone-4	1297-1311	80	37	33	116	2.3	18
Zone-5	1874-1898	66	33	36	87	2.4	15
Zone-6	1901-1944	60	69	35	95	2.3	14
Zone-7	2009-2033	81	22	25	88	2.4	22

4.3. Formation Temperature of the Reservoir Zones

The resistivity of the drilling mud (R_m), the resistivity of the mud filtrate (R_{mf}), and the resistivity of the formation water (R_w) were corrected with formation temperature to obtain accurate values. They are shown in the Table 4.3.

Table4.3. *Formation Temperature of Seven Zones of Well Sylhet #*

Zone	Depth Range, m (MD)	Average T_f (^oF)
Zone-1	428-450	91.59
Zone-2	488-500	93.41
Zone-3	1192-1263	117.78
Zone-4	1297-1311	120.33
Zone-5	1874-1898	139.56
Zone-6	1901-1944	140.77
Zone-7	2009-2033	144.04

Graphical Representation of average formation temperature and the middle depth of the different zones are shown in the Fig. 4.4 which shows that the formation temperature linearly increases with depth.

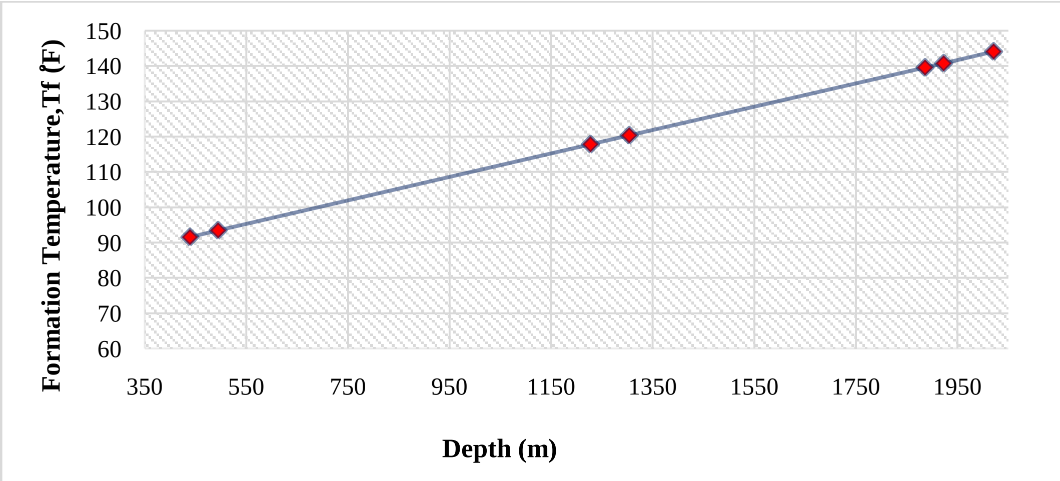

Fig4.4. *Depth vs average formation temperature of well Sylhet #*

4.4. Shale Volume

Shale has a vital effect in different reservoir properties. So, calculation of shale is very important. The percentage of average gamma ray index and average shale volume of seven zones are listed below in Table 4.4. It shows that Zone-3 is the cleanest zone among the seven zones.

Table4.4. *Gamma Ray Index (I_{GR}) and Shale volume (V_{sh}) of Seven Zones of the Well Sylhet #*

Zone	Depth Range, m (MD)	Gamma Ray Index (I_{GR}) Average (%)	Shale Volume (V_{sh}) Average (%)
Zone-1	428-450	47	26
Zone-2	488-500	31	13
Zone-3	1192-1263	25	9
Zone-4	1297-1311	45	26
Zone-5	1874-1898	28	12
Zone-6	1901-1944	32	14
Zone-7	2009-2033	56	32

4.5. Porosity Measurement from Different Porosity Log

Determination of porosity is very important to characterize a reservoir. It is an essential step to calculate water saturation. The average porosities determined from different methods are shown in Table 4.5 and Fig. 4.5. Combined porosity of Zone-1, Zone-2, Zone-3, Zone-4, Zone-5, Zone-6 and Zone-7 are 26%, 25%, 21%, 20%, 16%, 17% and 18% respectively.

Table4.5. *Average Porosity Values of Seven Zones of the Well Sylhet #*

Zone	Depth Range, m (MD)	Sonic (%)	Density (%)	Neutron (%)	Combined D-N (%)
Zone-1	428-450	43	32	15	26
Zone-2	488-500	48	29	19	25
Zone-3	1192-1263	34	25	15	21
Zone-4	1297-1311	36	22	17	20
Zone-5	1874-1898	21	16	15	16
Zone-6	1901-1944	30	19	14	17
Zone-7	2009-2033	21	13	21	18

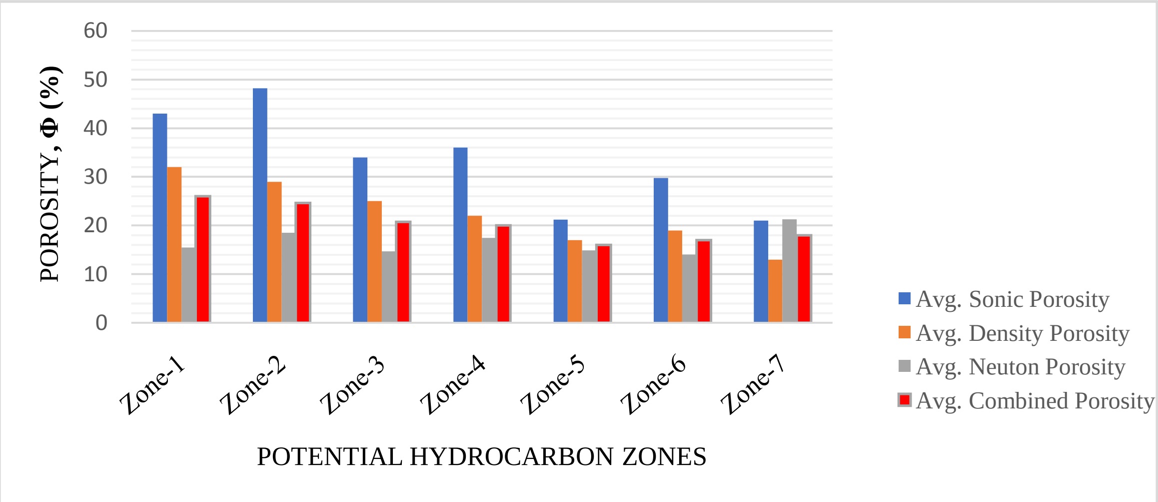

Fig4.5. *Comparison of avg. porosities of different potential hydrocarbon zones of well Sylhet #*

4.6. Water Saturation

Water saturation of the currently examined hydrocarbon bearing zones in the studied well was not determined from Archie's (1942) formula [25]. Because this formula is valid for clean sandstone and the values are much affected by incursion of shale and porosity [6]. Therefore, Simandoux (1963), Fertl (1975) and Schlumberger (1975) formula were used to calculate water saturation. We determined average water saturation S_w (avg.) for Zone-1, Zone-2, Zone-3, Zone-4, Zone-5, Zone-6 and Zone-7 were 25%, 32%, 23%, 24%, 37%, 24% and 38% respectively (Table 4.6 and Fig. 4.6). Among these, Zone-3 was the least water saturated compared to other zones.

Table4.6. *Water Saturation of Different Hydrocarbon Zones of the Well Sylhet #*

Gas Zone	Depth Range, m(MD)	S_w (Sd) (%)	S_w (Ft) (%)	S_w (Sc) (%)	S_w (Avg.) (%)
Zone-1	428-450	31	17	27	25
Zone-2	488-500	35	29	33	32
Zone-3	1192-1263	24	25	20	23
Zone-4	1297-1311	29	16	25	24
Zone-5	1874-1898	42	31	40	37
Zone-6	1901-1944	30	17	27	24
Zone-7	2009-2033	44	34	37	38

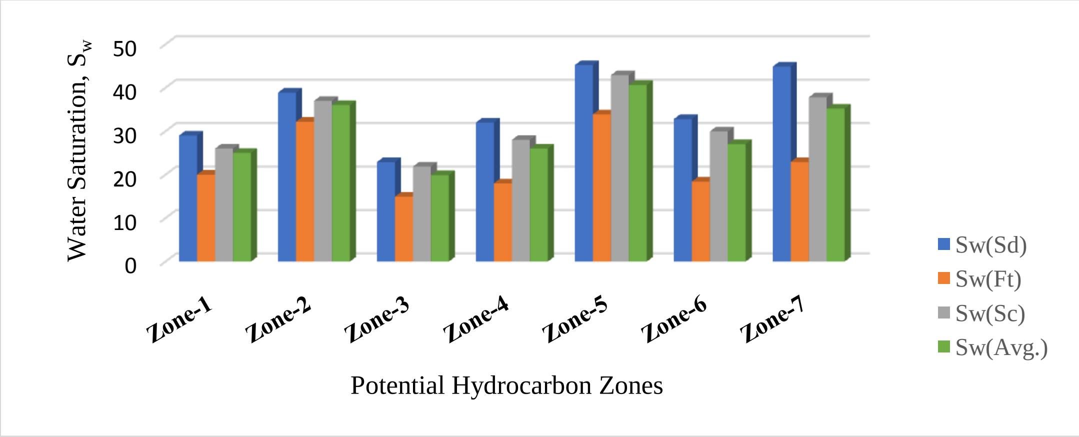

Fig4.6. *Comparison of water saturations (Sw) by using Fertl (1975), Schlumberger (1975), Simandoux (1963) formulas of different zones of well Sylhet #*

4.7. Hydrocarbon Saturation

Sufficient amount of hydrocarbon saturation is present in all the seven zones for hydrocarbon production. Although hydrocarbon saturation is the quantity of interest, water saturation is usually used because of its direct calculation in equations [9]. Hydrocarbon saturation was determined by the difference between unity and water saturation. We found that the average hydrocarbon saturation S_h (avg.) of hydrocarbon Zone-1, Zone-2, Zone-3, Zone-4, Zone-5, Zone-6 and Zone-7 of the Well Sylhet # were 75%, 68%, 77%, 76%, 63%, 76%, and 62%, respectively (Table 4.7 and Fig. 4.7).

Table4.7. *The Average Hydrocarbon Saturation of Different Hydrocarbon Zones of the Well Sylhet #*

Zones	Depth Range, m (MD)	S_h(Sd) (%)	S_h (Ft) (%)	S_h (Sc) (%)	S_h (Avg.) (%)
Zone-1	428-450	69	83	73	75
Zone-2	488-500	65	71	67	68
Zone-3	1192-1263	76	75	80	77
Zone-4	1297-1311	71	84	75	76
Zone-5	1874-1898	58	69	60	63
Zone-6	1901-1944	70	83	73	76
Zone-7	2009-2033	56	66	63	62

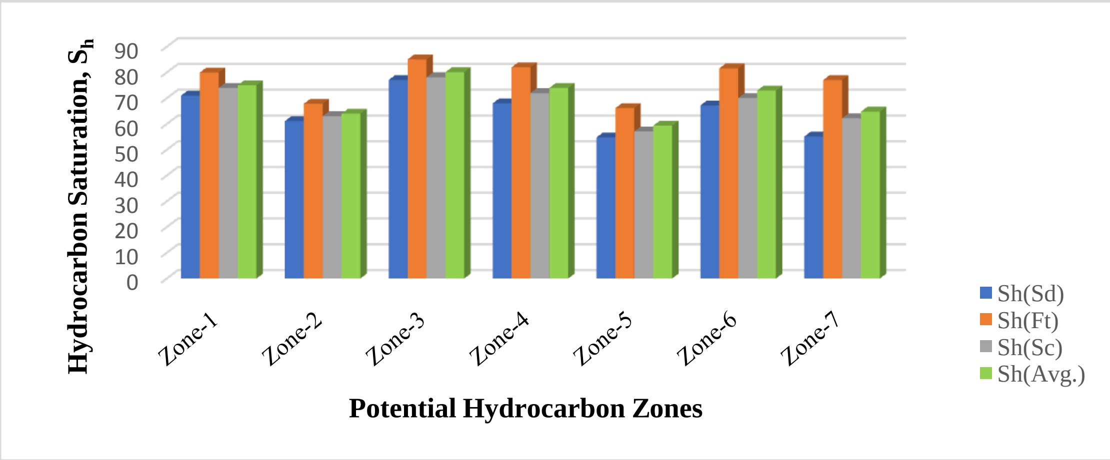

Fig4.7. *Comparison of hydrocarbon saturations (S_h) by using Fertl (1975), Schlumberger (1975), Simandoux (1963) and average hydrocarbon saturation of different zones of well Sylhet #*

4.8. Bulk Volume of Water

The values for bulk volume of water, calculated at several depths in the formations were very close to constant. There was some minor scattering. They indicated that they were at irreducible water saturation ($S_{w\ irr}$) [11]. Water in the uninvaded zone does not move because it is held on grains by capillary pressure [11]. Average bulk volume of water for seven zones are listed in Table 4.8.

4.9. Moveable Hydrocarbon Index

In seven HC bearing gas and oil zones, the moveable hydrocarbon index, S_w/S_{xo} is less than 0.7. So, hydrocarbons will move during invasion [11]. Average moveable hydrocarbon index for seven zones are listed in Table 4.8.

4.10. Permeability from Logs

Permeability of the seven zones exhibited good range that supported the reservoirs to be productive reservoirs. Among them Zone-1 shows best permeability and Zone-5 shows least permeability. Wyllie and Rose (1950), Coates and Dumanoir (1973) and Timur (1968) formula were used to calculate permeability. The average permeability of sever zones is shown in Table 4.8. Average permeability of seven zones are also compared in the Fig. 4.8 for the used formulas.

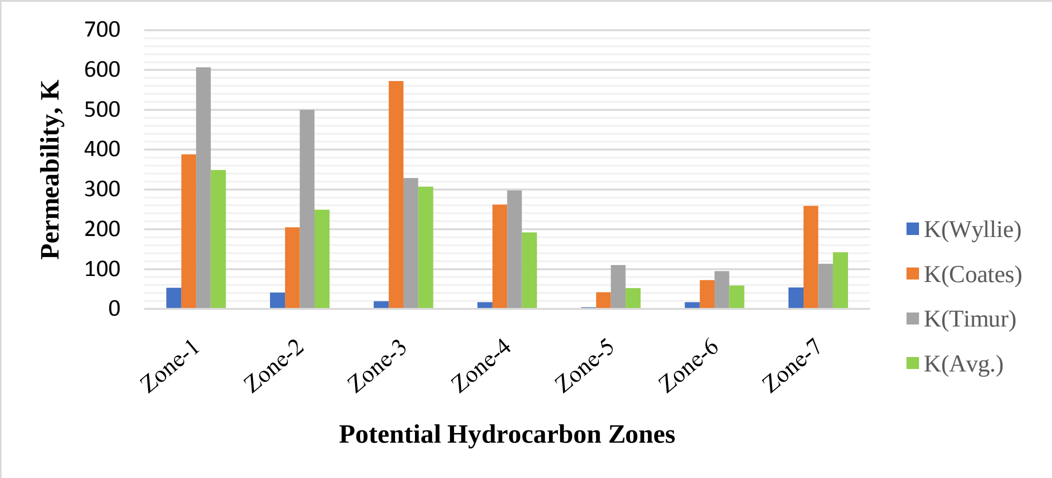

Fig4.8. *Comparison of the permeability using Wyllie and Rose (1950), Coates and Dumanoir (1973), Timur (1968) and average permeability of different zones of well Sylhet #*

The determined petrophysical parameters of seven hydrocarbon bearing zones of well Sylhet # are listed in Table 4.8. These calculated parameters are also graphically represented in Fig. 4.9 for the hydrocarbon bearing Zone-3 (Gas). The graphical representation of other zones is not shown here. It is clear that water saturation calculated from three different methods is relatively low in the specified sandstone area than the shaly area (Fig. 4.9). Permeability and hydrocarbon saturation are relatively high in this indicated clean sandstone zone (Fig 4.9). Shale volume is very low in the pointed out clean sandstone zone (Fig. 4.9). Moreover, Porosity is also relatively high in the indicated sandstone zone than the shaly regions (Fig. 4.9).

Table4.8. *Petrophysical Analysis Results of Seven Hydrocarbon (HC) Bearing Zones Identified in Sylhet #*

Zones	Depth	Thickness (m)	V_{sh} (%)	Φ_{ND} (%)	S_w (Sd)	S_w (Ft)	S_w (Sc)	S_w (Avg)	S_h (Sd)	S_h (Ft)	S_h (Sc)	S_h (Avg.)	BVW	S_w/S_{xo}	K (Wy)	K (Ct)	K (Ti)	K (Avg)
Zone-1	428-450	22	26	26	31	17	27	25	69	83	73	75	0.07	0.19	53	388	607	349
Zone-2	488-500	12	13	25	35	29	33	32	65	71	67	68	0.08	0.2	41	205	500	249
Zone-3	1194-1263	69	9	21	24	25	20	23	76	75	80	77	0.05	0.22	19	572	329	307
Zone-4	1297-1311	14	26	20	29	16	25	24	71	84	75	76	0.05	0.29	17	262	297	192
Zone-5	1874-1898	24	12	16	42	31	40	37	58	69	60	63	0.06	0.49	4	42	110	52
Zone-6	1901-1944	43	14	17	30	17	27	24	70	83	73	76	0.04	0.34	17	72	95	59
Zone-7	2009-2033	24	32	18	44	34	37	38	56	66	63	62	0.07	0.52	54	259	113	142

[Avg= Average; V_{sh} = Shale volume; Φ = Porosity; S_w= water saturation (%), Sc= Schlumberger (1975), Ft= Fertl (1975), Sd= Simandoux (1963); S_h= Hydrocarbon saturation (%); S_w/S_{xo}= Moveability; BVW= Bulk volume of water; K= Permeability (mD), Wy- Wyllie and Rose (1950), Ct- Coates and Dumanoir (1973)]

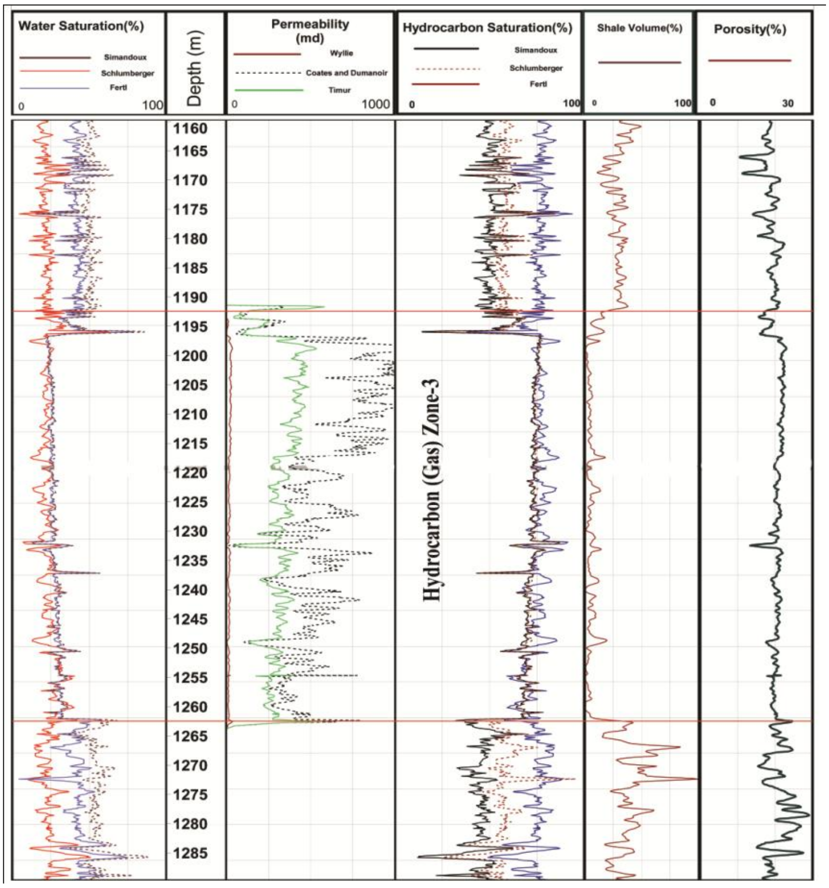

Fig4.9. *Graphical representation of the petrophysical parameters of hydrocarbon bearing Zone-3 (Gas) of well Sylhet #*

5. CONCLUSION

The present study of the well Sylhet # gives a petrophysical overview of the Sylhet Gas Field. The gas field consisting of several permeable zones are gas bearing, oil bearing and rest of the zones are water bearing. The average shale volume of the seven HC bearing zones are 9 to 32 percent. Remarkable GR values increasing or decreasing for the HC bearing formations of the well Sylhet-7 shows the presence of shale volume with the sand reservoir. From GR log data incorporate with other log data, it is evident that Zone-3 is the cleanest sandstone zone. The porosities of the seven zones are 26%, 25%, 21%, 20%, 16%, 17% and 18% respectively. According to Rider (1986) [26], the reservoir zones are at good to very good condition with respect to porosity. The average hydrocarbon saturations of the zones are 75%, 68%, 77%, 76%, 63%, 76% and 62% which is the indicative sufficient amount of hydrocarbon reserves. The average bulk volume of water values are very close to constant and they indicate that the zone is of a single rock type and at irreducible water saturation (S_{wirr}). The hydrocarbon movability index of all the zones are less than 0.7. It reveals that the hydrocarbon is movable in the reservoir. The average permeability values of the potential zones are 349 md, 249 md, 307 md, 192 md, 52 md, 59 md and 142 md respectively. By considering these average permeability, the hydrocarbon zones can be ranked good to very good reservoirs. This study suggests that the hydrocarbon reservoirs are potential for commercial gas (mainly) and oil (minor) production.

ABBREVIATIONS

AMSL	Above Mean Sea Level
BHC	Borehole Compensated Sonic Tool
BVW	Bulk volume water
BUET	Bangladesh University of Engineering and Technology
CALI	Caliper (in)
DRHO	Bulk Density Correction (g/cm3)
GR	Natural Gamma Ray (API units)
GR_{log}	Gamma ray reading from formation

GR_{max}	Gamma Ray Maximum
GR_{min}	Gamma Ray Minimum
HC	Hydrocarbon
I_{GR}	Gamma Ray Index
ILD	Deep Resistivity (ohm)
ILM	Medium Resistivity (ohm)
MSFL	Microspherically Focused Log (ohm)
mD	Milli Darcy
MD	Measured Depth
NPHI	Neutron Porosity (%)
Petrobangla	Bangladesh Oil, Gas and Mineral Corporation
PPL	Pakistan Petroleum Limited
PMRE	Petroleum and Mineral Resources Engineering
R_m	Resistivity of Drilling Mud
R_{mf}	Resistivity of Mud Filtrate
R_t	Resistivity of Uninvaded Zone
R_w	Resistivity of Formation Water
R_{xo}	Resistivity of Flushed Zone
$R_{t\ irr}$	Deep resistivity from a zone at irreducible water saturation
RHOB	Bulk Density (g/cm3)
SGFL	Sylhet Gas Fields Limited (A Company of Petrobangla)
SP	Spontaneous or Self Potential
SSP	Static SP
S_h	Hydrocarbon Saturation
S_w	Water Saturation
$S_{w\ irr}$	Irreducible Water Saturation
S_{xo}	Water Saturation of Flushed Zone
V_{sh}	Shale Volume
TVD	True Vertical Depth
W	Constant
Φ	Porosity
Φ_s	Sonic-derived porosity
Φ_{Se}	Effective (shale-corrected) sonic porosity
Φ_D	Density Porosity
Φ_{Ne}	Shale-corrected neutron porosity
Φ_{De}	Shale-corrected density porosity
Φ_{Dsh}	Density porosity of a nearby shale
Φ_N	Neutron Porosity
Φ_{N-D}	Combined Neutron-Density Porosity
ρ_b	Bulk Density
ρ_{matrix}	Matrix Density
ρ_h	Hydrocarbon Density

REFERENCES

[1] Shofiqul, I. M., and Nusrat, J. L., Reservoir characterization of Habiganj gas field. International Journal of Oil, Gas and Coal Engineering, **1**(1), 7-15, (2013).

[2] Sakurai, S., Grimaldo-Suarez, F. M., Aguilera-Gomez, L. E., and Rodriguez-Larios, J. A., Estimate of lithology and net gas sand from wireline logs: Veracruz and Macuspana Basins, Mexico, Gulf Coast Asso. Geol. Soc. Transac, **52,** 871-881 (2002).

[3] Horsfall, O., Davies, D., and Davies, O., Hydrocarbon Reservoir Characterization Using Well Log in Niger Delta Basin of Nigeria, International Journal of Applied and Natural Sciences (IJANS), **4**(5), (2015).

[4] Asquith, G. B. and Gibson, R. C., Basic well log analysis for geologist, The AAPG, Houston, 1982.

[5] RPS Energy, Sylhet Geological Study, Prepared for Petrobangla, Dhaka, Bangladesh, (2009).

[6] Farhaduzzaman, M., Islam, M. A., Abdullah, W. H., and Dutta, J., Log based petrophysical analysis of mio-pliocene sandstone reservoir encountered in well Rashidpur 4 of Bengal Basin in Bangladesh, Bangladesh Journal of Scientific and Industrial Research, **51**(1), 23-34, (2016).

[7] Islam, A. R. M. T., and Islam, M. A., Evaluation of Gas Reservoir of the Meghna Gas Field, Bangladesh Using Wireline Log Interpretation, Universal Journal of Geoscience, **2**(2), 62-69, (2014).

[8] Islam, A. R. M. T., Habib, M. A., Islam, M. T., and Mita, M. R., Interpretation of wireline log data for reservoir characterization of the Rashidpur Gas Field, Bengal Basin, Bangladesh. IOSR Journal of Applied Geology and Geophysics (IOSR-JAGG), **1**(4), 47-54, (2013).

[9] Islam, M. S., Hosain, M., Jolly, Y. N., Hossain, M. S., Akter, S., and Kabir, J., Geochemical Analysis of the Reservoir Rocks of Surma Basin, Bangladesh. Geosciences, **5**(1), 1-7, (2015).

[10] Petrobangla, Petrobangla Annual Report 2013, Petrobangla, Dhaka, (2013).

[11] Asquith, G. B., Krygowski, D., and Gibson, C. R., Basic well log analysis (Vol. 16), Tulsa: American association of petroleum geologists, 2004.

[12] Enikanselu, P. A., and Adekanle, A., A Fortran Programme for Computing Formation (Connate) Water Resistivity from Spontaneous Potential Logs, American-Eurasian Journal of Scientific Research, **3**(2), 172-177, (2008).

[13] Wyllie, M. R. J., Gregory, A. R., and Gardner, G. H. F., An experimental investigation of factors affecting elastic wave velocities in porous media, Geophysics, **23**(3), 459-493, (1958).

[14] Atlas, D., Log Interpretation Charts, Houston, Dresser Industries. Inc., (1979).

[15] Schlumberger, A., A guide to well site interpretation of the gulf coast, Schlumberger Well Services, Houston., (1975).

[16] Fertl, W. H., Shaly-sand analysis in development wells, Soc, Professional Well Log Analysis, In 16th Ann Logging Symp. Trans., Paper A., (1975).

[17] Simandoux, P., Dielectric measurements on porous media, application to the measurements of water saturation: study of behavior of argillaceous formations. Revue de l'Institut Francais du Petrol, **18** (supplementary issue), 93-215, (1963).

[18] Wyllie, M. R. J., and Rose, W. D., Some theoretical considerations related to the quantitative evaluation of the physical characteristics of reservoir rock from electrical log data, Journal of Petroleum Technology, **2**(04), 105-110, (1950).

[19] Timur, A., An investigation of permeability, porosity, and residual water saturation relationships, In SPWLA 9th annual logging symposium, Society of Petrophysicists and Well-Log Analysts, January 8-17, (1968).

[20] Coates, G., and Dumanoir, J. L., A new approach to improve log-derived permeability; Society of Professional Well Log Analysis. In 14th Ann. Logging Symp. Trans. Paper R., (1973).

[21] Well log analysis for reservoir characterization. (2017, March 23). Retrieved from http:// wiki. aapg.org/ Well_log_analysis_for_reservoir_characterization.

[22] Ahammod, S., Hai, M. A., Islam, M. R., and Abu, S. M., Petro-Physical Analysis of Reservoir Rock Of Fenchuganj Gas Field (Well# 03) Using Wireline Log, **3**(8), 37, (2014).

[23] Atlas, D., Log review I. Dresser Atlas Division, Dresser Industries., (1974).

[24] Charts, Schlumberger Log Interpretation, Schlumberger Limited, New York., (2009).

[25] Archie, G. E., The electrical resistivity log as an aid in determining some reservoir characteristics, Transactions of the AIME, **146**(01), 54-62, (1942).

[26] Rider, M. H., The geological interpretation of well logs, Blackie, Glasgow., 1986.

Citation: *Abdullah Al Fatta et.al, (2018). Petrophysical Analysis of Sylhet Gas Field Using Well Logs and Associated Data from Well Sylhet #, Bangladesh***,** *International Journal of Petroleum and Petrochemical Engineering (IJPPE), 4(1), pp.55-69, DOI: http://dx.doi.org/10.20431/2454-7980.0401007*